Rare Earth-rich Cadmium Compounds $RE_{23}T_7Cd_4$ (T = Co, Ni, Ru, Rh, Ir, Pt)

Frank Tappe and Rainer Pöttgen

Institut für Anorganische und Analytische Chemie, Universität Münster, Corrensstraße 30, D-48149 Münster, Germany

Reprint requests to R. Pöttgen. E-mail: pottgen@uni-muenster.de

Z. Naturforsch. **2009**, *64b,* 184 – 188; received November 11, 2008

The rare earth-rich intermetallic compounds $RE_{23}T_7Cd_4$ (RE = La–Nd, Sm, Gd, Tb; T = Co, Ni, Ru, Rh, Ir, Pt) were synthesized by melting of the elements in sealed tantalum tubes in a high-frequency furnace. They crystallize with the $Pr_{23}Ir_7Mg_4$-type structure, space group $P6_3mc$, $Z = 2$. The structures of $La_{23}Pt_7Cd_4$ (a = 1025.4(2), c = 2319.5(5) pm, $wR2$ = 0.0425, 2587 F^2, 74 variables), $La_{23}Ru_{6.87(1)}Cd_4$ (a = 1015.0(2), c = 2282.8(4) pm, $wR2$ = 0.0383, 2459 F^2, 75 variables), and $Nd_{23}Rh_7Cd_4$ (a = 990.0(2), c = 2239.0(5) pm, $wR2$ = 0.0507, 2350 F^2, 74 variables) were refined from single crystal X-ray diffractometer data. Central structural motifs of the $RE_{23}T_7Cd_4$ compounds are transition metal-centered trigonal prisms of rare earth atoms and Cd_4 tetrahedra. The RE_6T prisms are condensed *via* common edges and corners, leading to three-dimensional networks. Typical interatomic distances in the prismatic network and in the Cd_4 tetrahedra are 295 – 313 pm La–Pt and 319 – 325 pm Cd–Cd, respectively (examplarily for $La_{23}Pt_7Cd_4$).

Key words: Intermetallics, Cadmium, Crystal Chemistry

Introduction

The rare earth (RE) metal-rich parts of the ternary phase diagrams RE-T-X (T = late transition metal; X = element of the 3rd, 4th, or 5th main group) have only scarcely been studied. The structures of the ternary compounds are often quite complex. A striking structural motif of such structures is a trigonal-prismatic coordination of the transition metal atoms, and often distinct, segregated substructures of the X component occur.

An interesting example is the family of $RE_{14}T_3In_3$ compounds [1, and refs. therein], where the In2 atoms build up dumb-bells (309 pm in $Y_{14}Ir_3In_3$) within the rare earth metal network. Even larger units have been observed in the cubic structure type Gd_4RhIn [2] where the indium atoms form tetrahedra (317 pm) which are well separated within the rare earth metal matrix. Interestingly, the same structure type has been observed with the rare structural motif of Mg_4 and Cd_4 tetrahedra for several series of RE_4TMg and RE_4TCd compounds [3, 4, and refs. therein]. Our recent phase analytical investigations in the rare earth metal-rich parts of the RE-T-Mg systems revealed the existence of another structure type with similar structural features.

Table 1. Lattice parameters (Guinier powder data) of the ternary cadmium compounds $RE_{23}T_7Cd_4$.

Compound		a (pm)	c (pm)	V (nm^3)
$RE_{23}Co_7Cd_4$	$La_{23}Co_7Cd_4$	1007.2(2)	2279.7(6)	2.0028
	$Ce_{23}Co_7Cd_4$	980.0(6)	2221.2(13)	1.8474
$RE_{23}Ni_7Cd_4$	$La_{23}Ni_7Cd_4$	1011.7(3)	2298.5(6)	2.0374
	$Ce_{23}Ni_7Cd_4$	992.4(2)	2252.9(8)	1.9215
	$Pr_{23}Ni_7Cd_4$	987.2(3)	2243.8(7)	1.8938
	$Nd_{23}Ni_7Cd_4$	979.1(2)	2226.7(6)	1.8486
$RE_{23}Ru_7Cd_4$	$La_{23}Ru_7Cd_4$	1015.0(2)	2282.8(4)	2.0367
	$Ce_{23}Ru_7Cd_4$	988.7(3)	2241.6(5)	1.8977
	$Pr_{23}Ru_7Cd_4$	992.7(2)	2236.4(7)	1.9086
	$Nd_{23}Ru_7Cd_4$	990.2(2)	2225.5(4)	1.8897
	$Sm_{23}Ru_7Cd_4$	980.9(2)	2204.5(8)	1.8369
$RE_{23}Rh_7Cd_4$	$La_{23}Rh_7Cd_4$	1012.5(2)	2291.0(4)	2.0340
	$Ce_{23}Rh_7Cd_4$	997.4(3)	2256.7(8)	1.9442
	$Pr_{23}Rh_7Cd_4$	992.9(2)	2248.1(5)	1.9194
	$Nd_{23}Rh_7Cd_4$	990.0(2)	2239.0(5)	1.9004
	$Sm_{23}Rh_7Cd_4$	983.7(2)	2223.5(4)	1.8633
	$Gd_{23}Rh_7Cd_4$	971.7(2)	2193.1(5)	1.7933
	$Tb_{23}Rh_7Cd_4$	967.7(4)	2177.6(12)	1.7660
$RE_{23}Ir_7Cd_4$	$La_{23}Ir_7Cd_4$	1017.5(2)	2292.4(4)	2.0554
	$Ce_{23}Ir_7Cd_4$	1000.0(2)	2257.4(5)	1.9550
	$Pr_{23}Ir_7Cd_4$	996.5(2)	2245.9(6)	1.9314
	$Nd_{23}Ir_7Cd_4$	991.8(2)	2234.4(4)	1.9034
	$Sm_{23}Ir_7Cd_4$	983.2(2)	2214.0(4)	1.8535
$RE_{23}Pt_7Cd_4$	$La_{23}Pt_7Cd_4$	1025.4(2)	2319.5(5)	2.1121
	$Ce_{23}Pt_7Cd_4$	1008.4(2)	2278.8(5)	2.0068
	$Pr_{23}Pt_7Cd_4$	1004.2(2)	2271.5(6)	1.9837
	$Nd_{23}Pt_7Cd_4$	999.6(2)	2260.8(5)	1.9563

Table 2. Crystal data and structure refinement for $La_{23}Pt_7Cd_4$, $La_{23}Ru_{6.87(1)}Cd_4$ and $Nd_{23}Rh_7Cd_4$ (space group $P6_3mc$, $Z = 2$).

Empirical formula	$La_{23}Pt_7Cd_4$	$La_{23}Ru_{6.87(1)}Cd_4$	$Nd_{23}Rh_7Cd_4$
Unit cell dimensions	Table 1	Table 1	Table 1
Molar mass, g mol^{-1}	5010.16	4338.88	4487.49
Calculated density, g cm^{-3}	7.88	7.08	7.84
Crystal size, μm^3	$20 \times 40 \times 60$	$20 \times 40 \times 60$	$10 \times 20 \times 60$
Transm. ratio (max/min)	0.361 / 0.116	0.403 / 0.133	0.608 / 0.336
Absorption coeff., mm^{-1}	47.7	28.0	35.9
Detector distance, mm	80	80	80
Exposure time, min	5	8	8
ω range; increment, deg	0 – 180; 1.0	0 – 180; 1.0	0 – 180; 1.0
Integr. param. A; B; EMS	13.0; 3.5; 0.012	13.0; 3.0; 0.012	13.5; 3.5; 0.012
$F(000)$, e	4098	3611	3774
θ range, deg	2 – 31	2 – 31	2 – 31
Range in *hkl*	$\pm$14, $\pm$14, $\pm$33	$\pm$14, $\pm$14, $\pm$33	$\pm$14, $\pm$14, $\pm$32
Total no. reflections	24204	15434	21913
Independent reflections / R_{int}	2587 / 0.0690	2459 / 0.0570	2350 / 0.1853
Reflections with $I \geq 2\sigma(I)/R_\sigma$	1935 / 0.0822	1869 / 0.0648	895 / 0.2690
Data / parameters	2587 / 74	2459 / 75	2350 / 74
Goodness-of-fit on F^2	0.670	0.722	0.467
Final $R1/wR2$ indices [$I \geq 2\sigma(I)$]	0.0272 / 0.0408	0.0244 / 0.0365	0.0335 / 0.0423
Final $R1/wR2$ indices (all data)	0.0412 / 0.0425	0.0402 / 0.0383	0.0973 / 0.0507
Flack parameter	0.027(9)	0.02(3)	0.13(6)
Extinction coefficient	0.000150(4)	0.000241(6)	0.000101(5)
Largest diff. peak / hole, e Å^{-3}	4.54 / $-$2.42	1.12 / $-$1.48	3.15 / $-$2.43

The $RE_{23}T_7Mg_4$ compounds with T = Ni, Rh, Ir) [5 – 7] show the same transition metal-centered trigonal RE_6T prisms, but with a different connectivity pattern, besides slightly elongated, isolated Mg_4 tetrahedra (Mg–Mg 312 – 317 pm in $Nd_{23}Rh_7Mg_4$). Herein we report on the synthesis and structure elucidation of the corresponding cadmium compounds which again have a rare structural motif with Cd_4 tetrahedra.

Experimental Section

Synthesis

Starting materials for the synthesis of the $RE_{23}T_7Cd_4$ samples were ingots of the rare earth metals (Johnson Matthey or smart elements), cobalt powder (Sigma-Aldrich, 100 mesh), nickel powder (Johnson Matthey), ruthenium, rhodium, iridium, and platinum powder (Degussa-Hüls or Heraeus), and a cadmium rod (Johnson-Matthey), all with stated purities better than 99.9 %. Pieces of the rare earth ingots were first arc-melted [8] to small buttons under an argon atmosphere. The argon was purified before with molecular sieves, silica gel, and titanium sponge (900 K). Next the rare earth metal buttons, the transition metal powders and pieces of the cadmium rod (23 : 7 : 4 atomic ratio) were sealed in tantalum tubes under an argon pressure of *ca.* 700 mbar. The ampoules were placed in a water-cooled sample chamber of a high-frequency furnace (Hüttinger Elektronik, Freiburg, Germany; type TIG 1.5/300 under flowing argon [9], first heated at about 1370 K, and then kept at that temperature for 5 min. The temperature was then lowered within 5 min. to 873 K, and the tubes were annealed for another 3 h. Finally the tubes were quenched to r. t. The temperature was controlled through a Sensor Therm Methis MS09 pyrometer with an accuracy of $\pm$30 K. All samples could easily be separated from the ampoules by mechanical fragmentation. No reaction with the container material was observed. The polycrystalline samples are stable in air over weeks.

EDX data

Semiquantitative EDX analyses on the crystals investigated on the diffractometer were carried out by use of a Leica 420i scanning electron microscope with the rare earth trifluorides, ruthenium, rhodium, platinum, and cadmium as standards. The experimentally observed compositions were close to the ideal ones. No impurity elements heavier than sodium (detection limit of the instrument) were found.

X-Ray diffraction

The polycrystalline samples were investigated *via* Guinier powder patterns (imaging plate detector, Fujifilm BAS-1800 read out system) using Cu$K_{\alpha 1}$ radiation and α-quartz (a = 491.30 and c = 540.46 pm) as an internal standard. The hexagonal lattice parameters (Table 1) were refined from the powder data by least-squares calculations. The correct indexing of the complex patterns was ensured through intensity calculations [10].

Small, irregularly shaped single crystals of $La_{23}Pt_7Cd_4$, $La_{23}Ru_7Cd_4$, and $Nd_{23}Rh_7Cd_4$ were selected from the

crushed annealed samples, and their quality was checked by Laue photographs on a Buerger camera (white Mo radiation). Intensity data were collected at r. t. by use of a Stoe IPDS-II imaging plate diffractometer in oscillation mode (graphite-monochromatized MoK_α radiation). Numerical absorption corrections were applied to the data sets. All relevant details concerning the data collections and evaluations are listed in Table 2.

Structure refinements

The isotypy of $La_{23}Pt_7Cd_4$, $La_{23}Ru_7Cd_4$, and $Nd_{23}Rh_7Cd_4$ with the hexagonal $Pr_{23}Ir_7Mg_4$ type [5], space group $P6_3mc$, was already evident from the Guinier patterns. The observed systematic extinctions of the three data sets were in agreement with those found in our previous work. The atomic positions of isotypic $Pr_{23}Ir_7Mg_4$ [5] were taken as starting parameters. The three structures were refined using SHELXL-97 [11] (full-matrix least-squares on F^2) with anisotropic atomic displacement parameters for all atoms. Since the structures of $Pr_{23}Ir_{6.81}Mg_4$ [5] and $Gd_{23}Rh_{6.86}Mg_4$ [7] showed small defects on the $T2$ sites, the occupancy parameters for all three crystals were refined in separate series of least-squares cycles. For $La_{23}Pt_7Cd_4$ and $Nd_{23}Rh_7Cd_4$ all sites were fully occupied within three standard deviations but again, for $La_{23}Ru_{6.87(1)}Cd_4$ the Ru2 site showed an occupancy of only 95.6(6) %. Refinement of the correct absolute structure was ensured through calculation of the Flack parameter [12, 13]. The final difference Fourier syntheses were flat (Table 2). The positional parameters and interatomic distances are listed in Tables 3 and 4.

Further details of the crystal structure investigations may be obtained from Fachinformationszentrum Karlsruhe, 76344 Eggenstein-Leopoldshafen, Germany (fax: +49-7247-808-666; e-mail: crysdata@fiz-karlsruhe.de, http://www.fiz-informationsdienste.de/en/DB/icsd/depot_anforderung.html) on quoting the deposition numbers CSD-420068 ($La_{23}Pt_7Cd_4$), CSD-420067 ($La_{23}Ru_{6.87(2)}Cd_4$), and CSD-420066 ($Nd_{23}Rh_7Cd_4$).

Discussion

Twenty-seven new rare earth metal-rich cadmium intermetallics $RE_{23}T_7Cd_4$ with the transition metals T = Co, Ni, Ru, Rh, Ir, and Pt have been synthesized and structurally characterized. These compounds crystallize with the hexagonal $Pr_{23}Ir_7Mg_4$-type structure [5], space group $P6_3mc$. Similar to the series of the isotypic magnesium compounds, for cadmium the $Pr_{23}Ir_7Mg_4$-type compounds exist only for the larger rare earth elements, while the cubic Gd_4RhIn type [2] is formed for the smaller ones [4].

Table 3. Atomic coordinates and isotropic displacement parameters (pm^2) for $La_{23}Pt_7Cd_4$, $La_{23}Ru_{6.87(1)}Cd_4$ and $Nd_{23}Rh_7Cd_4$. U_{eq} is defined as one third of the trace of the orthogonalized U_{ij} tensor. The Ru2 site of $La_{23}Ru_{6.87(1)}Cd_4$ is occupied only by 95.6(6) %.

Atom	W.-position	x	y	z	U_{eq}
$La_{23}Pt_7Cd_4$					
La1	6*c*	0.12735(6)	$-x$	0.13677(4)	107(2)
La2	6*c*	0.19999(7)	$-x$	0.28364(4)	99(2)
La3	6*c*	0.20544(7)	$-x$	0.44511(4)	134(3)
La4	6*c*	0.21078(8)	$-x$	0.99068(4)	143(3)
La5	6*c*	0.53967(7)	$-x$	0.08521(5)	112(2)
La6	6*c*	0.54377(6)	$-x$	0.35614(4)	133(2)
La7	2*b*	1/3	2/3	0.14332(8)	100(3)
La8	2*a*	0	0	0.99385(8)	106(4)
La9	6*c*	0.79452(7)	$-x$	0.22089(5)	116(2)
Pt1	6*c*	0.47822(4)	$-x$	0.21169(3)	105(1)
Pt2	6*c*	0.85805(5)	$-x$	0.06320(3)	125(2)
Pt3	2*b*	1/3	2/3	0.36120(5)	121(3)
Cd1	6*c*	0.89439(8)	$-x$	0.36247(7)	157(3)
Cd2	2*a*	0	0	0.25100(12)	170(5)
$La_{23}Ru_{6.87(1)}Cd_4$					
La1	6*c*	0.12659(4)	$-x$	0.13480(4)	126(1)
La2	6*c*	0.20415(5)	$-x$	0.28197(3)	110(2)
La3	6*c*	0.20738(5)	$-x$	0.44787(3)	116(2)
La4	6*c*	0.20785(5)	$-x$	0.99056(4)	154(2)
La5	6*c*	0.54121(5)	$-x$	0.08622(4)	117(2)
La6	6*c*	0.54020(4)	$-x$	0.35476(4)	134(2)
La7	2*b*	1/3	2/3	0.14722(6)	109(3)
La8	2*a*	0	0	0.99776(7)	119(3)
La9	6*c*	0.79385(5)	$-x$	0.21986(5)	119(2)
Ru1	6*c*	0.48343(6)	$-x$	0.21148(6)	156(2)
Ru2	6*c*	0.85340(6)	$-x$	0.06037(6)	165(4)
Ru3	2*b*	1/3	2/3	0.3700(1)	154(4)
Cd1	6*c*	0.89547(5)	$-x$	0.36211(5)	129(2)
Cd2	2*a*	0	0	0.25062(9)	130(4)
$Nd_{23}Rh_7Cd_4$					
Nd1	6*c*	0.12720(14)	$-x$	0.13602(9)	93(4)
Nd2	6*c*	0.20067(15)	$-x$	0.28273(8)	80(4)
Nd3	6*c*	0.20753(15)	$-x$	0.44615(8)	100(5)
Nd4	6*c*	0.21040(17)	$-x$	0.99030(9)	122(6)
Nd5	6*c*	0.54012(15)	$-x$	0.08491(10)	100(4)
Nd6	6*c*	0.54259(13)	$-x$	0.35640(9)	95(5)
Nd7	2*b*	1/3	2/3	0.14550(16)	103(7)
Nd8	2*a*	0	0	0.99494(16)	86(8)
Nd9	6*c*	0.79371(16)	$-x$	0.22033(12)	91(5)
Rh1	6*c*	0.47915(16)	$-x$	0.21130(12)	88(6)
Rh2	6*c*	0.85721(19)	$-x$	0.06262(12)	112(7)
Rh3	2*b*	1/3	2/3	0.3638(3)	93(10)
Cd1	6*c*	0.89437(15)	$-x$	0.36282(14)	75(5)
Cd2	2*a*	0	0	0.2507(2)	55(9)

For most of the six series, the unit cell volumes decrease with increasing ordering number of the rare earth element as expected from the lanthanoid contraction. The only exception is $Ce_{23}Ru_7Cd_4$ (Table 1) which shows a strong anomaly for the lattice parameter a, even smaller than the a lattice parameter of the praseodymium compound. In contrast, the c parameter

Table 4. Interatomic distances (pm) of $La_{23}Pt_7Cd_4$, $La_{23}Ru_{6.87(1)}Cd_4$, and $Nd_{23}Rh_7Cd_4$, calculated with the powder lattice parameters. Standard deviations are all equal or smaller than 0.5 pm.

$La_{23}Pt_7Cd_4$			$La_{23}Ru_{6.87(1)}Cd_4$			$Nd_{23}Rh_7Cd_4$		
La1:	2 Pt2	294.6	La1:	2 Ru2	295.7	Nd1:	2 Rh2	284.8
	1 Cd2	348.4		1 Cd2	345.6		1 Cd2	336.8
	1 La2	364.3		1 La4	358.9		1 Nd2	351.8
	1 La7	366.1		1 La2	362.6		1 Nd7	354.1
	2 Pt1	368.9		1 La7	364.5		1 Nd4	356.1
	1 La4	369.8		2 Ru1	369.4		2 Rh1	357.1
	2 La9	374.0		2 La9	371.4		2 Nd9	362.2
	2 La5	385.2		2 La5	381.0		2 Nd5	372.1
	2 La1	391.8		1 La8	383.9		2 Nd1	377.8
	1 La8	401.3		2 La1	385.5		1 Nd8	383.9
La2:	1 Pt3	297.4	La2:	2 Ru1	295.2	Nd2:	2 Rh1	288.0
	2 Pt1	298.7		1 Ru3	303.2		1 Rh3	291.0
	2 Cd1	358.0		2 La6	359.0		2 Cd1	347.9
	1 Cd2	363.2		2 Cd1	360.7		1 Cd2	351.5
	1 La1	364.3		1 La1	362.6		1 Nd1	351.8
	2 La6	368.2		1 Cd2	366.0		2 Nd6	355.1
	1 La3	374.7		1 La3	378.8		1 Nd3	366.1
	2 La9	388.5		1 La7	382.4		2 Nd9	375.9
	1 La7	402.5		2 La9	387.5		1 Nd7	382.3
	2 La2	410.2		2 La2	393.4		2 Nd2	394.0
La3:	1 Pt2	296.2	La3:	1 Ru2	278.1	Nd3:	1 Rh2	283.4
	1 Pt3	299.1		1 Ru3	284.0		1 Rh3	283.8
	2 Cd1	369.6		2 Cd1	371.5		2 Cd1	360.3
	1 La2	374.7		2 La4	377.8		1 Nd2	366.1
	1 La8	382.0		1 La2	378.8		2 Nd4	371.7
	2 La4	384.5		1 La8	382.0		2 Nd6	371.8
	2 La6	386.0		2 La6	382.0		1 Nd8	372.3
	2 La3	393.4		2 La3	383.5		2 Nd3	373.6
	2 La5	396.0		2 La5	385.5		2 Nd5	378.6
La4:	1 Cd1	351.2	La4:	1 Cd1	344.9	Nd4:	1 Cd1	337.3
	1 La1	369.8		1 La1	358.9		1 Nd1	356.1
	2 Pt2	371.0		2 Ru2	362.2		2 Rh2	357.8
	1 La8	374.4		1 La8	365.8		1 Nd8	360.9
	2 La4	377.0		2 La3	377.8		2 Nd4	365.1
	2 La6	380.6		2 La6	381.0		2 Nd6	367.1
	2 La3	384.5		2 La4	382.1		2 Nd3	371.7
	2 La5	387.3		2 La5	386.4		2 Nd5	374.6
	1 La7	415.6		1 La7	420.2		1 Nd7	406.4
La5:	2 Pt2	303.9	La5:	2 Ru2	295.8	Nd5:	2 Rh2	292.3
	1 Pt1	313.0		1 Ru1	303.4		1 Rh1	301.7
	2 La1	385.2		2 La9	377.4		2 Nd1	372.1
	2 La4	387.3		2 La1	381.0		2 Nd9	373.1
	2 La9	387.6		2 La5	382.0		2 Nd4	374.6
	1 La7	390.5		2 La3	385.5		2 Nd5	375.8
	2 La5	390.7		2 La4	386.4		2 Nd3	378.6
	2 La3	396.0		1 La7	391.1		1 Nd7	379.7
La6:	2 Cd1	350.9	La6:	1 Ru1	342.0	Nd6:	2 Cd1	338.9
	1 Pt1	354.7		2 Cd1	349.4		1 Rh1	342.6
	2 La2	368.1		2 La2	359.0		2 Nd2	355.1
	1 Pt3	373.9		1 Ru3	365.3		1 Rh3	359.2
	2 La6	378.1		2 La9	380.2		2 Nd4	367.1
	2 La4	380.7		2 La4	381.0		2 Nd6	368.5
	2 La9	384.8		2 La3	382.0		2 Nd3	371.8
	2 La3	386.0		2 La6	385.1		2 Nd9	373.1
La7:	3 Pt1	302.3	La7:	3 Ru1	301.9	Nd7:	3 Rh1	290.2
	3 La1	366.1		3 La1	364.6		3 Nd1	354.1
	3 La5	390.5		3 La2	382.4		3 Nd5	379.7
	3 La2	402.5		3 La5	391.1		3 Nd2	382.3
	3 La4	415.6		3 La4	420.2		3 Nd4	406.4
La8:	3 Pt2	299.1	La8:	3 Ru2	294.7	Nd8:	3 Rh2	288.0
	3 Cd1	357.8		3 Cd1	360.1		3 Cd1	346.9
	3 La4	374.4		3 La4	365.8		3 Nd4	360.9
	3 La3	382.0		3 La3	382.0		3 Nd3	372.3
	3 La1	401.3		3 La1	383.9		3 Nd1	383.9
La9:	2 Pt1	296.7	La9:	2 Ru1	286.5	Nd9:	2 Rh1	285.0
	1 Cd2	371.6		1 Cd2	369.2		1 Cd2	360.2
	1 Cd1	373.2		1 Cd1	370.6		2 Nd1	362.2
	2 La1	374.0		2 La1	371.4		1 Cd1	362.7
	1 Pt2	382.8		2 La5	377.3		1 Rh2	369.5
	2 La6	384.8		1 Ru2	378.8		2 Nd6	373.1
	2 La5	387.6		2 La6	380.2		2 Nd5	373.1
	2 La2	388.5		2 La9	387.3		2 Nd2	375.9
	2 La9	393.3		2 La2	387.5		2 Nd9	377.3
Pt1:	2 La9	296.7	Ru1:	2 La9	286.5	Rh1:	2 Nd9	285.0
	2 La2	298.7		2 La2	295.2		2 Nd2	288.0
	1 La7	302.3		1 La7	302.0		1 Nd7	290.2
	1 La5	313.0		1 La5	303.4		1 Nd5	301.7
	1 La6	354.7		1 La6	342.0		1 Nd6	342.6
	2 La1	368.9		2 La1	369.4		2 Nd1	357.1
Pt2:	2 La1	294.6	Ru2:	1 La3	278.2	Rh2:	1 Nd3	283.4
	1 La3	296.2		1 La8	294.7		2 Nd1	284.8
	1 La8	299.1		2 La1	295.7		1 Nd8	288.0
	2 La5	303.9		2 La5	295.8		2 Nd5	292.3
	2 La4	371.0		2 La4	362.2		2 Nd4	357.8
	1 La9	382.8		1 La9	378.8		1 Nd9	369.5
Pt3:	3 La2	297.4	Ru3:	3 La3	284.0	Rh3:	3 Nd3	283.8
	3 La3	299.1		3 La2	303.3		3 Nd2	291.0
	3 La6	374.0		3 La6	365.3		3 Nd6	359.2
Cd1:	1 Cd2	319.4	Cd1:	1 Cd2	313.9	Cd1:	1 Cd2	309.6
	2 Cd1	324.9		2 Cd1	318.3		2 Cd1	313.7
	2 La6	350.9		1 La4	344.9		1 Nd4	337.3
	1 La4	351.2		2 La6	349.4		2 Nd6	338.9
	1 La8	357.8		1 La8	360.1		1 Nd8	346.9
	2 La2	358.0		2 La2	360.7		2 Nd2	347.9
	2 La3	369.6		1 La9	370.6		2 Nd3	360.3
	1 La9	373.2		2 La3	371.5		1 Nd9	362.7
Cd2:	3 Cd1	319.4	Cd2:	3 Cd1	313.9	Cd2:	3 Cd1	309.6
	3 La1	348.4		3 La1	345.6		3 Nd1	336.8
	3 La2	363.2		3 La2	366.0		3 Nd2	351.5
	3 La9	371.6		3 La9	369.2		3 Nd9	360.2

fits in between the lanthanum and the praseodymium compound. In view of the three crystallographically independent ruthenium sites, the precise reason for this anomaly is not yet known. Most likely strong Ce–Ru bonding, similar to that found in CeRuSn [14, 15] and Ce_2RuZn_4 [16], might be an explanation. Single crystal growth and magnetic susceptibility measurements on this compound are in progress in order to shed light on the peculiar crystal chemical data.

The crystal chemistry for this structure type and also a comparison with the structurally related RE_4TMg compounds have been considered in detail for the

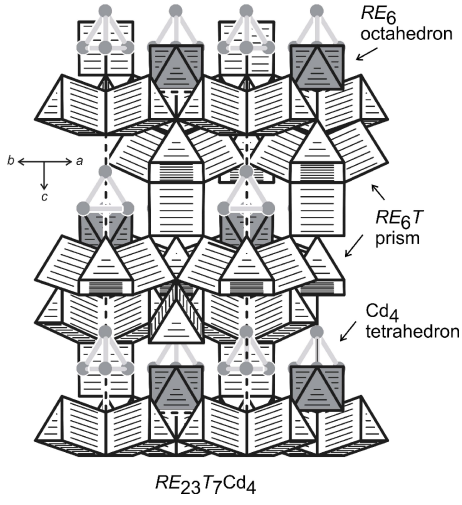

Fig. 1. View of the $RE_{23}T_7Cd_4$ structure approximately along the [110] direction. The network of condensed trigonal RE_6T prisms, the Cd_4 tetrahedra and the empty RE_6 octahedra (medium grey shading) are emphasized.

prototype $Pr_{23}Ir_7Mg_4$ [5]. Herein we exemplarily discuss the $La_{23}Pt_7Cd_4$ structure for the new series of cadmium compounds. A view of the $RE_{23}T_7Cd_4$ structure approximately along the [110] direction is presented in Fig. 1. The three crystallographically independent transition metal sites have all trigonal-prismatic rare earth metal coordination with comparatively short La–Pt distances in the range 295 – 313 pm, close to the sum of the covalent radii [17] of 298 pm. The La_6Pt prisms are condensed *via* common edges and corners, building a complex three-dimensional network which leaves voids for empty RE_6 octahedra and Cd_4 tetrahedra. The latter have Cd–Cd distances of 319 – 325 pm, which compare well with the Cd–Cd distances in *hcp* cadmium (6×298 and 6×329 pm) [18]. Tetrahedral cadmium units also occur in cadmium-rich phases $RECd_6$ [19, 20, and refs. therein], and similar ranges of Cd–Cd distances have been observed in several cadmium networks, *e. g.* the Cd_6 hexagons of $LaNiCd_2$ [21].

Acknowledgements

We thank Dipl.-Ing. U. Ch. Rodewald for the intensity data collections. This work was financially supported by the Deutsche Forschungsgemeinschaft.

[1] R. Zaremba, U. Ch. Rodewald, R. Pöttgen, *Z. Naturforsch.* **2007**, *62b*, 1574.
[2] R. Zaremba, U. Ch. Rodewald, R.-D. Hoffmann, R. Pöttgen, *Monatsh. Chem.* **2007**, *138*, 523.
[3] S. Tuncel, B. Chevalier, R. Pöttgen, *Z. Naturforsch.* **2008**, *63b*, 600.
[4] F. M. Schappacher, U. Ch. Rodewald, R. Pöttgen, *Z. Naturforsch.* **2008**, *63b*, 1127.
[5] U. Ch. Rodewald, S. Tuncel, B. Chevalier, R. Pöttgen, *Z. Anorg. Allg. Chem.* **2008**, *634*, 1011.
[6] S. Tuncel, W. Hermes, B. Chevalier, U. Ch. Rodewald, R. Pöttgen, *Z. Anorg. Allg. Chem.* **2008**, *634*, 2140.
[7] S. Linsinger, S. Tuncel, W. Hermes, M. Eul, B. Chevalier, R. Pöttgen, *Z. Anorg. Allg. Chem.*, in press.
[8] R. Pöttgen, Th. Gulden, A. Simon, *GIT Labor-Fachzeitschrift* **1999**, 43, 133.
[9] D. Kußmann, R.-D. Hoffmann, R. Pöttgen, *Z. Anorg. Allg. Chem.* **1998**, *624*, 1727.
[10] K. Yvon, W. Jeitschko, E. Parthé, *J. Appl. Crystallogr.* **1977**, *10*, 73.
[11] G. M. Sheldrick, SHELXL-97, Program for the Refinement of Crystal Structures, University of Göttingen, Göttingen (Germany) **1997**.
[12] H. D. Flack, G. Bernadinelli, *Acta Crystallogr.* **1999**, *A55*, 908.
[13] H. D. Flack, G. Bernadinelli, *J. Appl. Crystallogr.* **2000**, *33*, 1143.
[14] J. F. Riecken, W. Hermes, B. Chevalier, R.-D. Hoffmann, F. M. Schappacher, R. Pöttgen, *Z. Anorg. Allg. Chem.* **2007**, *633*, 1094.
[15] S. F. Matar, J. F. Riecken, B. Chevalier, R. Pöttgen, V. Eyert, *Phys. Rev. B* **2007**, *76*, 174434.
[16] R. Mishra, W. Hermes, U. Ch. Rodewald, R.-D. Hoffmann, R. Pöttgen, *Z. Anorg. Allg. Chem.* **2008**, *634*, 470.
[17] J. Emsley, *The Elements*, Oxford University Press, Oxford **1999**.
[18] J. Donohue, *The Structures of the Elements*, Wiley, New York, **1974**.
[19] S. Y. Piao, C. P. Gómez, S. Lidin, *Z. Naturforsch.* **2006**, *60b*, 644.
[20] S. Xia, S. Bobev, *Intermetallics* **2007**, *15*, 550.
[21] A. Doğan, D. Johrendt, R. Pöttgen, *Z. Anorg. Allg. Chem.* **2005**, *631*, 451.